Proc. Natl. Acad. Sci. USA
Vol. 92, pp. 9407–9411, September 1995
Cell Biology

Oligomeric structure of caveolin: Implications for caveolae membrane organization

MASSIMO SARGIACOMO*, PHILIPP E. SCHERER*, ZHAOLAN TANG, ERIC KÜBLER, KENNETH S. SONG, MITCHELL C. SANDERS, AND MICHAEL P. LISANTI†

The Whitehead Institute for Biomedical Research, 9 Cambridge Center, Cambridge, MA 02142-1479

Communicated by Martin Rodbell, National Institute of Environmental Health Sciences, Research Triangle Park, NC, June 5, 1995 (received for review April 13, 1995)

ABSTRACT **A 22-kDa protein, caveolin, is localized to the cytoplasmic surface of plasma membrane specializations called caveolae. We have proposed that caveolin may function as a scaffolding protein to organize and concentrate signaling molecules within caveolae. Here, we show that caveolin interacts with itself to form homooligomers. Electron microscopic visualization of these purified caveolin homooligomers demonstrates that they appear as individual spherical particles. By using recombinant expression of caveolin as a glutathione *S*-transferase fusion protein, we have defined a region of caveolin's cytoplasmic N-terminal domain that mediates these caveolin–caveolin interactions. We suggest that caveolin homooligomers may function to concentrate caveolin-interacting molecules within caveolae. In this regard, it may be useful to think of caveolin homooligomers as "fishing lures" with multiple "hooks" or attachment sites for caveolin-interacting molecules.**

Caveolae are plasma membrane specializations (1). Caveolin, a 21- to 24-kDa integral membrane protein, has been identified as a principal component of caveolae membranes *in vivo* (2, 3). Purification of caveolin-rich membrane domains reveals several distinct classes of signaling molecules (3–6). These include heterotrimeric guanine nucleotide binding proteins (G proteins; α and $\beta\gamma$ subunits), Src-like kinases, protein kinase Cα, and Rap GTPases. Based on these observations, we have proposed (1) that caveolin may function as a scaffolding protein to organize and concentrate inactive signaling molecules within caveolae membranes—for activation by appropriate receptors. This caveolae signaling hypothesis states that "compartmentalization of certain cytoplasmic signaling molecules within caveolae could allow efficient and rapid coupling of activated receptors to more than one effector system" (1). In support of this view, inactive G α subunits interact directly with caveolin in a 1:1 stoichiometry—holding them in an inactive conformation (7). Thus, knowledge of the subunit structure of caveolin is important for understanding how caveolin might function to organize or concentrate G α subunits and other signaling molecules within caveolae membranes.

In this report, we show that caveolin interacts with itself to form a discrete high molecular mass oligomer. As caveolin also interacts with G α subunits, self oligomerization of caveolin could provide a means for concentrating trimeric G proteins and other caveolin-interacting molecules within caveolae. The existence of caveolin homooligomers complexed with inactive G proteins could explain the observations of Rodbell and colleagues (8), who observed that inactive G proteins exist as high molecular mass oligomeric complexes and that activated G proteins dissociate to monomers. Similarly, activated G proteins fail to interact with recombinant caveolin (7).

The publication costs of this article were defrayed in part by page charge payment. This article must therefore be hereby marked "*advertisement*" in accordance with 18 U.S.C. §1734 solely to indicate this fact.

MATERIALS & METHODS

Materials. Antibodies to carbonic anhydrase IV and glutathione *S*-transferase (GST) were gifts of W. S. Sly (St. Louis University) and R. Young (Whitehead Institute), respectively. Molecular weight standards for velocity gradient centrifugation were from Sigma. Conditions for the culture, cell surface biotinylation, and metabolic labeling of MDCK cells were as described (9). Caveolin-rich membrane domains (4, 5, 9), adipocyte plasma membrane fractions (6), and GST–caveolin fusion proteins (7, 10) were purified as described.

Velocity Gradient Centrifugation. Samples were dissociated by incubation with 500 μl of Mes-buffered saline (MBS; 25 mM Mes, pH 6.5/0.15 M NaCl)/60 mM octyl glucoside. Solubilized material was then loaded atop a 5–30% linear sucrose gradient (4.3 ml) and centrifuged at 50,000 rpm ($\approx$340,000 $\times$ *g*) for 16 hr in a SW60 rotor (Beckman). Note that the entire gradient was prepared with MBS/60 mM octyl glucoside. After centrifugation, thirteen 380-μl gradient fractions were collected from above. To better estimate the molecular mass of GST–caveolin-(61–101), we modified our velocity gradients to accommodate its larger size. Samples were loaded atop a 5–40% linear sucrose gradient (4.3 ml) and centrifuged at 50,000 rpm ($\approx$340,000 $\times$ *g*) for 10 hr in a SW60 rotor. Gradient fractions were separated by SDS/PAGE, transferred to nitrocellulose, and subjected to immunoblot analysis with anti-caveolin IgG (2297; diluted 1:400) or anti-GST antibodies (diluted 1:1000). Biotinylated proteins were detected with iodinated streptavidin (9). Samples were also subjected to low-angle platinum shadowing (4, 9) and two-dimensional gel electrophoresis (11).

Chemical Cross-Linking. Samples were cross-linked with bis(sulfosuccinimidyl)suberate (BS^3; Pierce) in 50 μl of 0.2 M sodium borate (pH 8.5) for 30 min at 4°C as suggested by the manufacturer. For caveolin homooligomers, samples contained 60 mM octyl glucoside, and plasma membrane fractions were cross-linked in the absence of detergent. After cross-linking, reactions were quenched and samples were analyzed by SDS/PAGE (5–12% polyacrylamide gels). Cross-linked products of phosphorylase *b* (Sigma) were used to estimate the molecular mass of caveolin.

Gel-Filtration Chromatography. A Sephacryl S-400 HR column (total volume, 7.7 ml) was preequilibrated with 5 vol of column buffer {10 mM Tris·HCl, pH 8.0/0.2 M NaCl/30 mM HECAMEG [methyl-6-*O*-(*N*-heptylcarbamoyl) α-D-glucopyranoside; Calbiochem]/0.1% NaN_3} and chromatographed by FPLC (LCC-500 Plus; Pharmacia) at a flow rate of 0.25 ml/min.

RESULTS

Characterization of Caveolin Homooligomers. The predicted molecular mass of a single caveolin molecule is $\approx$20.6 kDa,

Abbreviations: GST, glutathione *S*-transferase; G protein, guanine nucleotide binding protein; BS^3, bis(sulfosuccinimidyl)suberate.

*M.S. and P.E.S. contributed equally to this work.

†To whom reprint requests should be addressed.

although it migrates in SDS/PAGE gels with an apparent mass of 21–24 kDa. To assess the oligomeric state of caveolin and its associated cell surface components, we solubilized caveolin-rich domains with octyl glucoside and subjected this material to velocity gradient centrifugation. By comparison with the migration of molecular weight standards, most MDCK cell surface labeled components of caveolin-rich domains migrated as monomers and were effectively separated from caveolin. However, caveolin migrated as a high molecular mass complex of 300–325 kDa (Fig. 1*A*, peak fractions 9 and 10). No caveolin monomers were detectable. In addition, these velocity gradients effectively separated caveolin from a 21- to 24-kDa MDCK biotinylated protein (12) that we had identified as a "cell surface form of caveolin" by its comigration in one-dimensional gels.

To further evaluate the generality of this phenomenon, we examined caveolin-rich domains purified from lung tissue. To effectively follow the protein components of these domains, we subjected them to *in vitro* biotinylation, which allows the detection of picogram quantities of protein. Caveolin-rich domains were first dissociated, biotinylated in solution, and subjected to velocity gradient centrifugation. Under these conditions, caveolin also migrated as a high molecular mass complex (Fig. 1*B*, peak fractions 9 and 10). As caveolin represents the major, if not the sole, protein component of this molecular complex, caveolin appears to exist as a large stable homooligomer of well-defined molecular mass. In contrast, CD36 (an 88-kDa transmembrane protein) and carbonic anhydrase IV (a 40- to 50-kDa glycosylphosphatidylinositol-linked protein)—other major hydrophobic membrane proteins of caveolin-rich domains (5)—migrated with a mass expected of monomers or homodimers in these velocity gradients and were effectively separated from caveolin (Fig. 1*C*).

Although caveolin represents the major protein in fractions 9–12 of these velocity gradients, an additional 21- to 24-kDa protein might be masked by comigration with caveolin in one-dimensional SDS/PAGE. To evaluate this possibility, we isolated caveolin-rich domains from MDCK cells after steady-

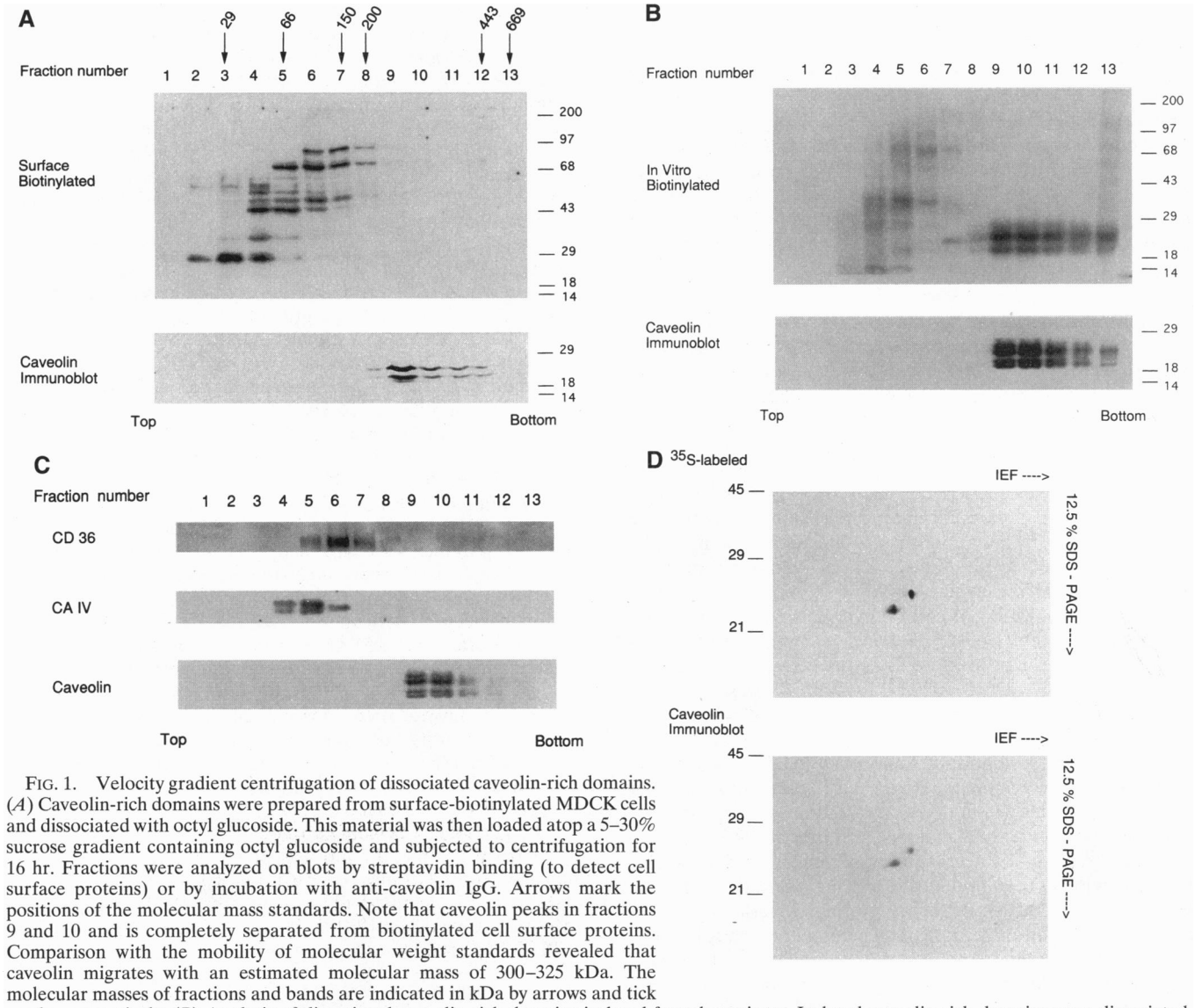

FIG. 1. Velocity gradient centrifugation of dissociated caveolin-rich domains. (*A*) Caveolin-rich domains were prepared from surface-biotinylated MDCK cells and dissociated with octyl glucoside. This material was then loaded atop a 5–30% sucrose gradient containing octyl glucoside and subjected to centrifugation for 16 hr. Fractions were analyzed on blots by streptavidin binding (to detect cell surface proteins) or by incubation with anti-caveolin IgG. Arrows mark the positions of the molecular mass standards. Note that caveolin peaks in fractions 9 and 10 and is completely separated from biotinylated cell surface proteins. Comparison with the mobility of molecular weight standards revealed that caveolin migrates with an estimated molecular mass of 300–325 kDa. The molecular masses of fractions and bands are indicated in kDa by arrows and tick marks, respectively. (*B*) Analysis of dissociated caveolin-rich domains isolated from lung tissue. Isolated caveolin-rich domains were dissociated, biotinylated in solution, and subjected to velocity gradient centrifugation as in *A*. The total protein pattern was visualized by streptavidin binding; caveolin was detected by immunoblot analysis. Caveolin appears to be the most abundant protein in fractions 9–12. (*C*) Immunoblot analysis with antibodies to CD36 (peak fractions 5–6) or carbonic anhydrase IV (CA IV; peak fractions 4 and 5) reveals that these proteins were effectively separated from caveolin (peak fractions 9 and 10). (*D*) Caveolin is the only 21- to 24-kDa species in the 300- to 325-kDa complex. MDCK cells were subjected to steady-state metabolic labeling with ^{35}S-labeled methionine and cysteine and used to prepare caveolin-rich domains. After dissociation, these domains were fractionated by velocity gradient centrifugation in octyl glucoside as in *A*. Fractions 9 and 10, expected to contain caveolin, were pooled and analyzed by two-dimensional gel electrophoresis. After separation, two major ^{35}S-labeled spots were identified that corresponded exactly to the position of caveolin as determined by immunoblot analysis with anti-caveolin IgG.

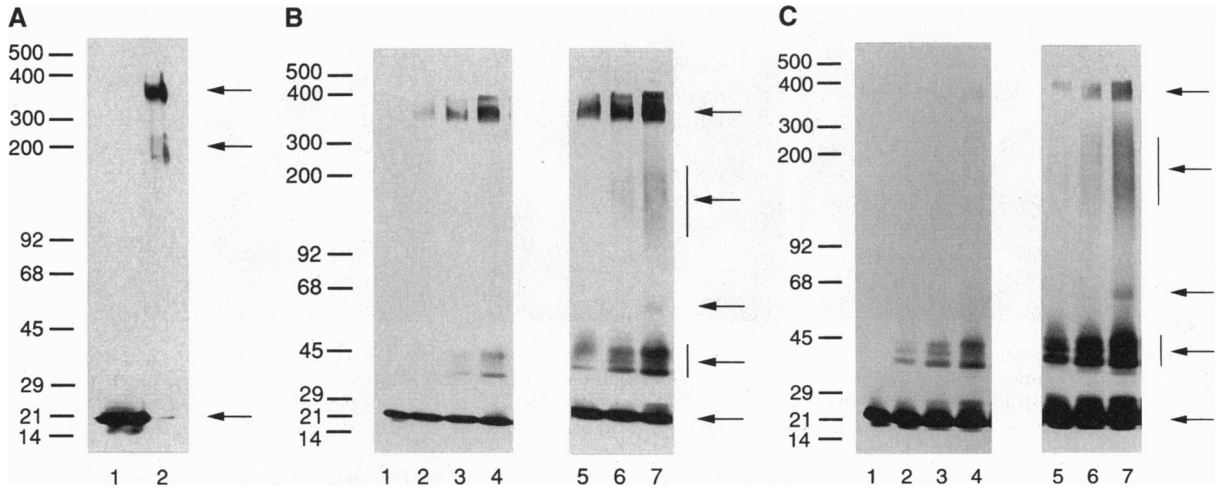

FIG. 2. High molecular mass caveolin homooligomers visualized by SDS/PAGE. (*A*) Detection of an SDS-resistant ≈350-kDa form of caveolin. Caveolin homooligomers (fractions 9 and 10) were dissolved in sample buffer containing SDS and 2-mercaptoethanol, subjected to SDS/PAGE, and transferred to nitrocellulose. Lanes: 1, heat-treated prior to loading; 2, without boiling. Note that heat-dissociated caveolin migrated as a monomer (21–24 kDa) and undissociated caveolin migrated with an apparent molecular mass of ≈350 kDa (major species) and ≈200 kDa (minor species) (arrows). Molecular masses in kDa are shown. (*B*) Chemical cross-linking of caveolin. Caveolin homooligomers were subjected to chemical cross-linking with a homobifunctional agent, BS^3, that reacts with primary amino groups. Lanes: 1, untreated control; 2–4, BS^3 at 0.1, 0.2, and 0.5 mg/ml, respectively; 5–7, a longer exposure of lanes 2–4. Vertical lines to the right indicate heterogeneously cross-linked species. (*C*) Plasma membrane fractions isolated in the absence of detergent were subjected to chemical cross-linking without detergent solubilization. Lanes: 1, untreated control; 2–4, BS^3 at 0.1, 0.2, and 0.5 mg/ml, respectively; 5–7, a longer exposure of lanes 2–4. In *A–C*, caveolin was visualized after transfer to nitrocellulose by immunoblot analysis with anti-caveolin IgG.

state metabolic labeling with ^{35}S-labeled amino acids. These domains were dissociated and fractionated by velocity gradient centrifugation. Fractions 9 and 10 were pooled and analyzed by SDS/PAGE, revealing only two major bands in the 21- to 24-kDa region. These fractions were also separated by two-dimensional gel electrophoresis, revealing two ^{35}S-labeled spots. These spots correspond exactly to the position of caveolin as revealed by immunoblot analysis with anti-caveolin IgG (Fig. 1*D*). Thus, caveolin appears to exist as a large homooligomer as (*i*) caveolin migrates in velocity gradients as a high molecular mass complex and (*ii*) complexes of this size can be shown to contain only proteins that are 21–24 kDa and are immunoreactive with anti-caveolin IgG.

We used denaturing SDS/PAGE analysis to independently study caveolin homooligomers. We observed that caveolin homooligomers are resistant to dissociation by a mixture of SDS and 2-mercaptoethanol, except at elevated temperatures (boiling at 100°C for 2 min), suggesting a very strong interaction between individual caveolin monomers. Fig. 2*A* shows the electrophoretic mobilities in SDS/PAGE gels (5–12% polyacrylamide gradient gels) of caveolin homooligomers and heat-dissociated caveolin monomers. Caveolin homooligomers migrated as a single major ≈350-kDa species and as a minor ≈200-kDa species, while caveolin monomers migrated with a mass of 21–24 kDa.

Chemical cross-linking also reveals ≈350-kDa caveolin homooligomers but allows the visualization of an array of smaller cross-linked intermediate species because of the inefficiencies inherent in the cross-linking approach. Two major cross-linked products were observed—a doublet of 40–44 kDa and a high molecular mass oligomer of ≈350 kDa; other cross-linked species at 65–66 kDa and 100–300 kDa were also seen (Fig. 2*B*). Based on the monomeric molecular weight of caveolin (21–24 kDa), these cross-linked products represent dimers, trimers, tetramers, and higher order oligomers of caveolin. Note that a doublet of 40–44 kDa is expected as two major isoforms of caveolin can be separated by SDS/PAGE (α-caveolin, 24 kDa, and β-caveolin, 21 kDa). In some experiments, this 40- to 44-kDa doublet was further resolved into three bands. This may reflect homo- and heterodimers of the two major isoforms of caveolin. Importantly, similar results were obtained when purified plasma membrane fractions were used as the substrate for cross-linking in the absence of detergent (Fig. 2*C*).

To examine the ultrastructure of purified caveolin homooligomers, we visualized these complexes by electron microscopy by using low-angle platinum shadowing. In the presence of octyl glucoside, caveolin homooligomers appeared as individual globular particles of 4–6 nm (Fig. 3*A Left*). When octyl glucoside is removed by dialysis, these globular particles self-associate to form larger structures (nonlinear polymers ≈25 nm in diameter, arrowheads) and become sedimentable in the microcentrifuge (Fig. 3*A Right*). Assembly appears to result from the side-by-side packing of individual caveolin homooligomers. Caveolin-rich membrane domains—used as the starting material for caveolin purification—are also coated with these globular subunits (Fig. 3*B*). As caveolin is a principal component of the caveolae membrane *in vivo*, these results have implications for understanding the construction of caveolae membranes.

Functional Mapping of a Caveolin Region that Contains Oligomerization Activity. Caveolin can be divided into three domains: an N-terminal region (the N domain, residues 1–101), a membrane spanning region (the TM domain, residues 102–134), and a C-terminal region (the C domain, residues 135–178) (13, 14). Both the N and C domains of caveolin remain entirely cytoplasmic (10, 15).

To localize the homooligomerization activity to a given caveolin domain, we expressed these three domains (N, TM, and C) separately as GST fusion proteins. GST–caveolin fusion proteins remained soluble after purification and did not sediment in the microcentrifuge (14,000 × g; 30 min at 4°C), indicating that they do not behave as insoluble aggregates. To assess their oligomeric state, each purified GST–caveolin fusion protein was subjected to velocity gradient centrifugation under the same conditions used for endogenous caveolin. Gradient fractions were examined by SDS/PAGE and immunoblot analysis with anti-GST antibodies. Although GST–TM-caveolin and GST–C-caveolin comigrated with GST alone (a homodimer of ≈52 kDa) (data not shown), GST–N-caveolin migrated as a high molecular mass oligomer (Fig. 4*A*). It is important to note that the N domain of caveolin (residues 1–101) does not contain any Cys residues, indicating that

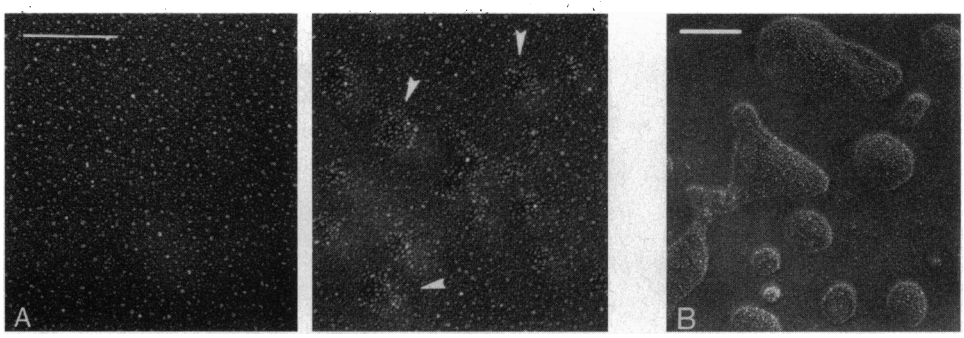

FIG. 3. Low-angle platinum shadowing of purified caveolin homooligomers. (*A*) Purified ≈350-kDa caveolin homooligomers prepared by velocity gradient centrifugation (pooled fractions 9 and 10). (*Left*) Homooligomers appear as individual 4- to 6-nm globular particles. (*Right*) Homooligomers after dialysis to remove octyl glucoside. (Bar = 0.05 μm.) (*B*) Caveolin-rich membrane domains used as the starting material are shown for comparison. (Bar = 0.1 μm.) Caveolin homooligomers and caveolin-rich domains were prepared from lung tissue.

its homooligomerization activity is independent of disulfide bond formation.

The observation that the cytoplasmic N domain of caveolin encodes information specifying homooligomerization prompted us to perform deletion mutagenesis of this region (residues 1–101). Deletion mutants endcoding residues 1–21 and 1–61 did not form high-order oligomers, while residues 61–101 retained this homooligomerization activity (Fig. 4*A*).

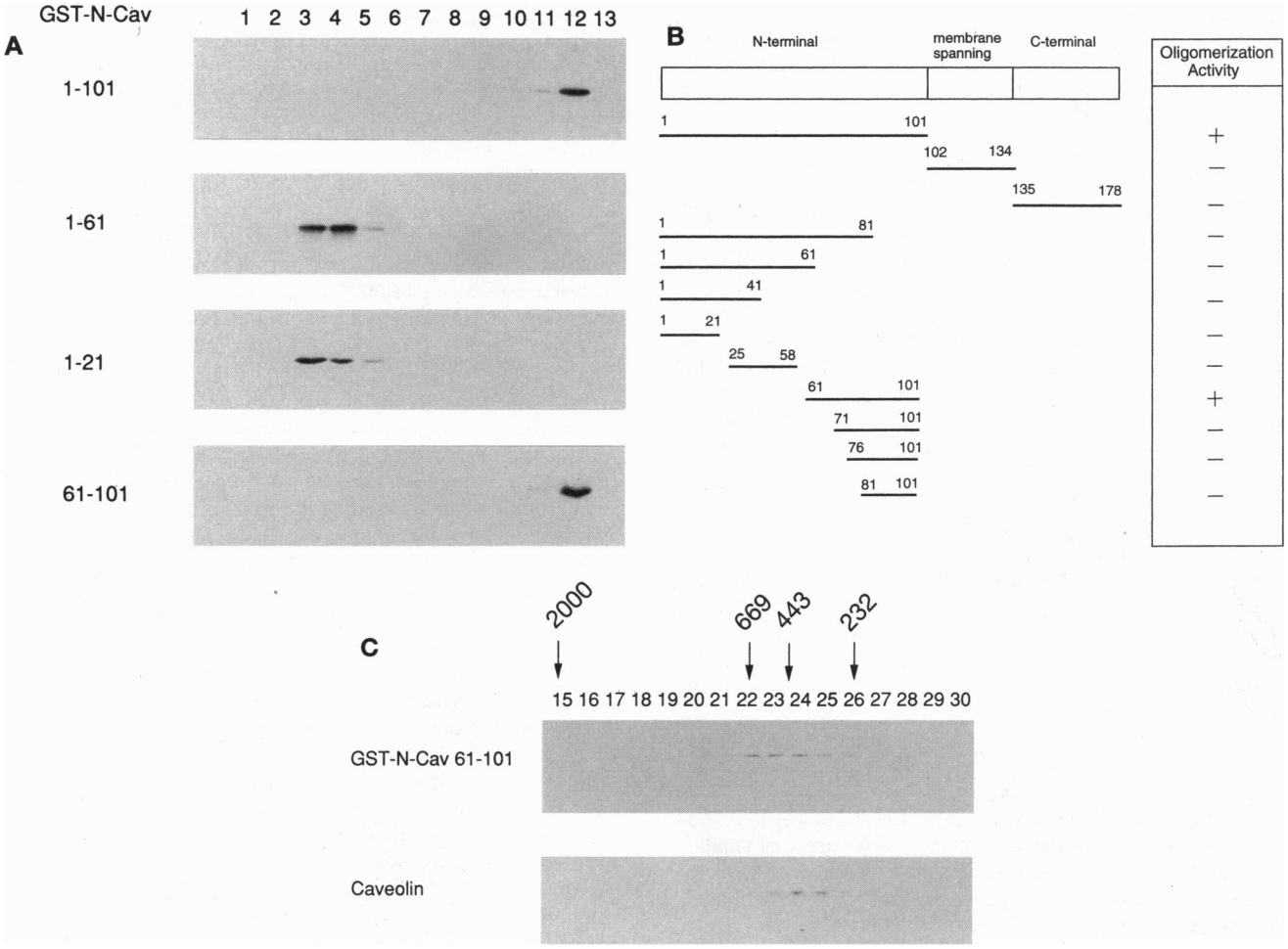

FIG. 4. Deletion analysis of the N-terminal domain of caveolin. (*A*) Each affinity-purified GST–caveolin (GST–N-Cav) fusion protein was subjected to velocity gradient centrifugation as described in Fig. 1*A*. Note that only GST–N-caveolin-(1–101) and GST–N-caveolin-(61–101) form high molecular mass oligomers. GST-tagged proteins were visualized by immunoblot analysis with anti-GST antibodies. (*B*) Summary of the properties of the GST–caveolin fusion proteins. Numbers at ends refer to amino acid positions within caveolin. A plus under activity denotes that a given caveolin region is sufficient to confer high-order oligomerization upon GST. (*C*) Gel filtration chromatography of GST–N-caveolin-(61–101) and endogenous caveolin on Sephacryl S-400 HR. Approximately 100 fractions were collected; fractions containing a given protein were first identified on dot blots and subsequently subjected to SDS/PAGE analysis. Fraction numbers are as indicated. Arrows mark the positions of the molecular mass standards: blue dextran (2000 kDa), thyroglobulin (669 kDa), apoferritin (443 kDa), and catalase (232 kDa). (*Upper*) GST–N-caveolin-(61–101) (peak fractions 23 and 24). (*Lower*) Endogenous caveolin purified from lung tissue (peak fractions 24 and 25). Proteins were visualized by immunoblot analysis with anti-GST or anti-caveolin IgG, respectively. Both GST–caveolin-(61–101) and endogenous caveolin migrated as high molecular mass homooligomers; no monomeric forms were detected.

Smaller deletion mutants encoding caveolin residues 71–101, 76–101, or 81–101 did not form high-order oligomers. These findings are summarized schematically in Fig. 4*B*.

To estimate the molecular mass of GST–N-caveolin-(61–101), we slightly modified our velocity gradients to accommodate its larger size so that it would migrate toward the middle of the gradient (5–40% sucrose; 10 hr). Under these conditions, GST–N-caveolin-(61–101) migrated as a discrete species (peak fraction 7; ≈80% of the fusion protein was recovered in this fraction) with an estimated molecular mass of 400–450 kDa, compared with standards such as apoferritin (443 kDa; peak fractions 7 and 8); none of the GST–N-caveolin-(61–101) was pelleted in these gradients (data not shown). Virtually identical estimates of molecular mass were obtained by gel-filtration chromatography on Sephacryl S-400 HR; the migration of endogenous caveolin homooligomers is shown for comparison (Fig. 4*C*).

Recently, we have determined that the two isoforms of caveolin differ in their N-terminal protein sequence: α-caveolin contains residues 1–178, while β-caveolin contains residues 32–178 (10). Thus, both isoforms contain the oligomerization residues 61–101, and herein we observe that (*i*) both isoforms comigrate as high molecular mass oligomers in velocity gradients (Fig. 1) and (*ii*) chemical cross-linking of intact plasma membranes reveals hetero- and homodimers of these two isoforms (Fig. 2 *B* and *C*). Thus, caveolin residues 1–31 are not required for homooligomerization as we have confirmed with GST fusion proteins.

DISCUSSION

Previous morphological studies have suggested that the characteristic cytoplasmic surface of caveolae membranes is composed of integral membrane protein subunits. Caveolin, a 22-kDa integral membrane protein, has been identified as a principal component of these caveolae subunits by immunoelectron microscopy labeling (2). These studies directly establish that caveolin exists as a large discrete complex within the membranes of intact cells (2) and also predict that caveolin might be expected to oligomerize with itself or other proteins.

Herein, we have shown that caveolin interacts with itself to form homooligomers. Caveolin behaves as a single major high molecular mass species based on a variety of methods. For example, caveolin is eluted specifically as a discrete peak in fractions 24 and 25 of a gel-filtration column between molecular mass standards of 232 kDa and 443 kDa (Fig. 4).

Endogenous caveolin homooligomers behave as complexes with a molecular mass of ≈350 kDa although caveolin has a monomeric mass by SDS/PAGE of 24–25 kDa. Similarly, GST fusion proteins containing the oligomerization region (caveolin residues 61–101) behave as complexes with a molecular mass of ≈450 kDa although they have a monomeric molecular mass by SDS/PAGE of ≈32 kDa. As such, each of these complexes should contain ≈14 monomers. Thus, residues 61–101 can direct the formation of high molecular mass complexes of the same relative stoichiometry as endogenous caveolin homooligomers.

What could be the structural basis for this oligomerization? The α/β coiled fold is built from a primary sequence repeat of ≈30 aa that assumes an α-helix at its N-terminal end and a β-conformation at its C-terminal end. The β-strands of each of these units then align in a parallel fashion forming a ring-like structure containing 16 individual units (16). Similarly, our results suggest that a 41-aa region of caveolin (residues 61–101) may assume the same secondary structure (based on primary sequence predictions) and that this region can form oligomers of the same relative stochiometry (≈14 individual units).

We have suggested (1) that caveolin may function as an "organizing or clustering factor" for concentrating signaling molecules within caveolae membranes. This is based on the observation that partially purified caveolin exists as a heterooligomeric complex with signaling molecules (3–5). How does this relate to our current observations? If each caveolin molecule binds a given signaling molecule, then caveolin would sort or concentrate signaling molecules simply by existing as a homooligomer within caveolae. In support of this hypothesis, (*i*) both caveolin and G proteins are concentrated within purified caveolae membranes up to 8-fold relative to total plasma membrane (3) and (*ii*) caveolin interacts with inactive G α subunits in a 1:1 stoichiometry (7).

As caveolin is a major v-Src substrate (13), our current findings may also have implications for understanding v-Src transformation. Tyrosine-phosphorylated caveolin homooligomers could potentially serve as oligomeric docking sites for SH2-domain signaling molecules during v-Src transformation—much like activated growth factor receptors that oligomerize, undergo tyrosine phosphorylation, and recruit SH2-domain-containing proteins to the cytoplasmic surface of the plasma membrane.

We thank H. Lodish, D. Baltimore, D. Sabatini, and R. G. W. Anderson for review of the manuscript and P. Reilly for rotary shadowing. This work was supported by a National Institutes of Health FIRST award (GM-50443 to M.P.L.) and a grant from the W. M. Keck Foundation to the Whitehead Fellows program. P.E.S. is funded by a fellowship from the Swiss National Science Foundation and National Institutes of Health grants (GM-49516 and DK-47618) to H. Lodish.

1. Lisanti M. P., Scherer, P., Tang, Z.-L. & Sargiacomo, M. (1994) *Trends Cell Biol.* **4,** 231–235.
2. Rothberg, K., Heuser, J., Donzell, W., Ying, Y., Glenney, J. R. & Anderson, R. G. W. (1992) *Cell* **68,** 673–682.
3. Chang, W. J., Ying, Y., Rothberg, K., Hooper, N., Turner, A., Gambliel, H., De Gunzburg, J., Mumby, S., Gilman, A. & Anderson, R. G. W. (1994) *J. Cell Biol.* **126,** 127–138.
4. Sargiacomo, M., Sudol, M., Tang, Z.-L. & Lisanti, M. P. (1993) *J. Cell Biol.* **122,** 789–807.
5. Lisanti, M. P., Scherer, P. E., Vidugiriene, J., Tang, Z.-L., Hermanoski-Vosatka, A., Tu, Y.-H., Cook, R. F. & Sargiacomo, M. (1994) *J. Cell Biol.* **126,** 111–126.
6. Scherer, P. E., Lisanti, M. P., Baldini, G., Sargiacomo, M., Corley-Mastick, C. & Lodish, H. F. (1994) *J. Cell Biol.* **127,** 1233–1243.
7. Li, S., Okamoto, T., Chun, M., Sargiacomo, M., Casanova, J. E., Hansen, S., Nishimoto, I. & Lisanti, M. P. (1995) *J. Biol. Chem.* **270,** 15693–15701.
8. Jahangeer, S. & Rodbell, M. (1993) *Proc. Natl. Acad. Sci. USA* **90,** 8782–8786.
9. Lisanti, M. P., Tang, Z.-T., Scherer, P. & Sargiacomo, M. (1995) *Methods Enzymol.* **250,** 655–668.
10. Scherer, P. E., Tang, Z.-L., Chun, M. C., Sargiacomo, M., Lodish, H. F. & Lisanti, M. P. (1995) *J. Biol. Chem.* **270,** 16395–16401.
11. O'Farrell, P. H. (1975) *J. Biol. Chem.* **250,** 4007–4021.
12. Lisanti, M. P., Tang, Z.-L. & Sargiacomo, M. (1993) *J. Cell Biol.* **123,** 595–604.
13. Glenney, J. R. & Soppet, D. (1992) *Proc. Natl. Acad. Sci. USA* **89,** 10517–10521.
14. Kurzchalia, T., Dupree, P., Parton, R. G., Kellner, R., Virta, H., Lehnert, M. & Simons, K. (1992) *J. Cell Biol.* **118,** 1003–1014.
15. Dupree, P., Parton, R. G., Raposo, G., Kurzchalia, T. V. & Simons, K. (1993) *EMBO J.* **12,** 1597–1605.
16. Yoder, M. D. & Jurnak, F. (1995) *FASEB J.* **9,** 335–342.